

Supporting information

Preparation of γ -Fe₂O₃-1. Coating process with APTS.

Briefly, the APTES was added to ferrofluid (molar ratio 1:0.3) in 200 mL of methanol under continuous stirring. Then 200 mL of glycerine was added under vigorous stirring and the oil-phase was extracted. The aqueous phase was evaporated under vacuum and ethanol and acetone were added to extract the excess of functional group reagent. Finally the ferrofluid was washed with water and acetone.

Preparation of γ -Fe₂O₃-2. Coating process with TEOS.

Ethanol and ammonia (4.12 and 0.212 mol respectively) were added to the γ -Fe₂O₃ ferrofluid, raising the pH up to 11. After 20 min of sonication, 6 mg of tetraethylorthosilicate (TEOS) was added and left for 4 hours under sonication. The solvents were removed under reduced pressure.

FTIR characterization of γ -Fe₂O₃ nanoparticles

Fourier Transform Infrared (FTIR) spectroscopy in a Thermo Nicolet Nexus spectrometer in the transmission mode using the KBr pellet method.

The surface chemical changes of the magnetic nanoparticles, γ -Fe₂O₃-0, γ -Fe₂O₃-1 and γ -Fe₂O₃-2 were studied using FTIR (Fig. S1). All the materials exhibited characteristic absorption bands of maghemite at 634 and 582 cm⁻¹ corresponding to the ν (Fe-O) deformations in the tetrahedral and the octahedral sites. γ -Fe₂O₃-0 sample shows a strong band at ca. 1380 cm⁻¹ which is assigned to the ν (O-N-O) stretching mode of the nitrate used during the synthesis process. These bands are also present in the aminosilane coated samples where the new bands are present at ca. 3390 (ν (NH)), 2930 (ν (CH₂)) and 1295 cm⁻¹ (ω (CH₂)). The siloxane bonds ν (Si-O-Si) were detected at ca. 1120 and 1030 cm⁻¹ which are present in the SiO₂ coated sample.

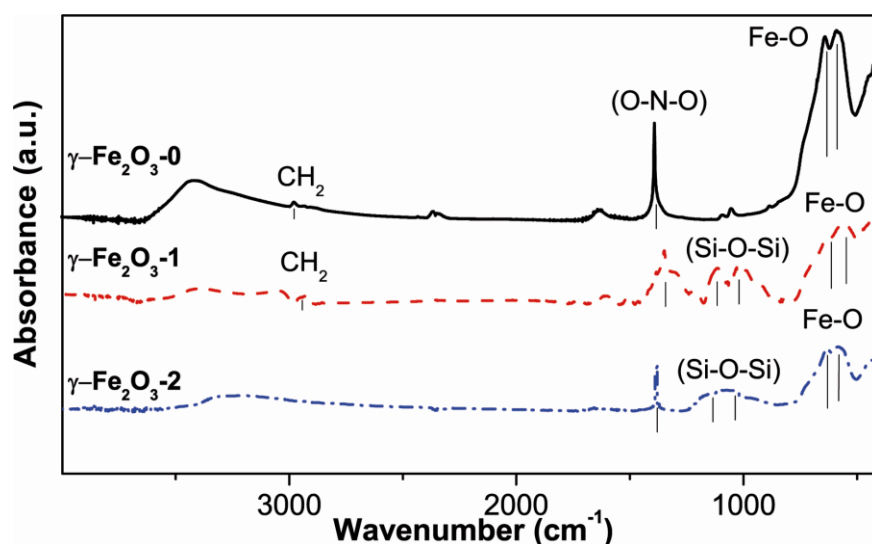


Figure S1. FTIR spectra of maghemite nanoparticles ($\gamma\text{-Fe}_2\text{O}_3\text{-0}$), APTES functionalized maghemite nanoparticles ($\gamma\text{-Fe}_2\text{O}_3\text{-1}$) and silica coated maghemite nanoparticles ($\gamma\text{-Fe}_2\text{O}_3\text{-2}$).

XRD studies on magnetic mesoporous silica spheres

Figure S2 displays the low angle XRD patterns of the samples after the encapsulation attempt into mesoporous silica spheres. The diffraction pattern of $\gamma\text{-Fe}_2\text{O}_3\text{-0@}$ shows a maximum, which can be indexed to the (10) reflection of 2D-hexagonal structure similar to MCM-41 mesoporous silica material, with unit cell parameter $a = 4.2$ nm. In the case of samples $\gamma\text{-Fe}_2\text{O}_3\text{-1@}$ and $\gamma\text{-Fe}_2\text{O}_3\text{-2@}$, this maximum is poorly defined indicating a defective mesoporous structure.

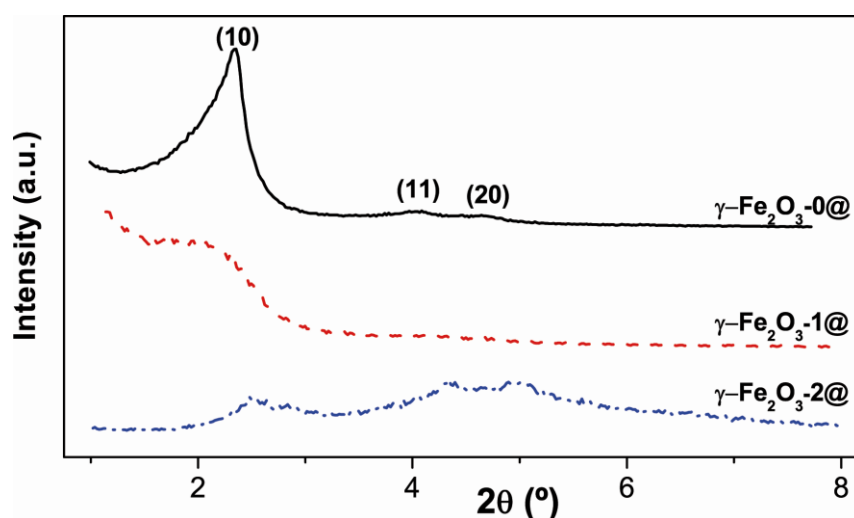


Figure S2. Low angle XRD patterns of the $\gamma\text{-Fe}_2\text{O}_3\text{-n@}$ (after the encapsulation process).

N₂ adsorption porosimetry studies on magnetic mesoporous silica spheres

The textural properties of the dried samples were determined by N₂ adsorption/desorption analyses at -196 °C with a Micrometrics ASAP 2020 instrument (Micromeritics Co, Norcross, USA). In all cases, 100 mg of samples were degassed during 24 h at 100 °C under vacuum lower than 10⁻⁵ bar.

The textural properties of the materials after the encapsulation process were analyzed with nitrogen adsorption-desorption techniques. As it can be seen in Fig. S3, N₂ adsorption isotherms are characteristic of MCM-41 mesoporous materials, exhibiting type IV isotherms. These materials do not possess adsorption-desorption hysteresis, which could be due to a reversible capillary condensation-evaporation in mesopores. The γ -Fe₂O₃-0 @ isotherm shows the typical narrow step in the 0.1-0.3 relative pressure (p/p₀) range which is characteristic of mesopore pore size uniformity. The γ -Fe₂O₃-2@ and γ -Fe₂O₃-1@ materials exhibit also a high pore size uniformity but with ill-defined mesoporous structures as reflected in the low-angle XRD patterns (Fig. S2)

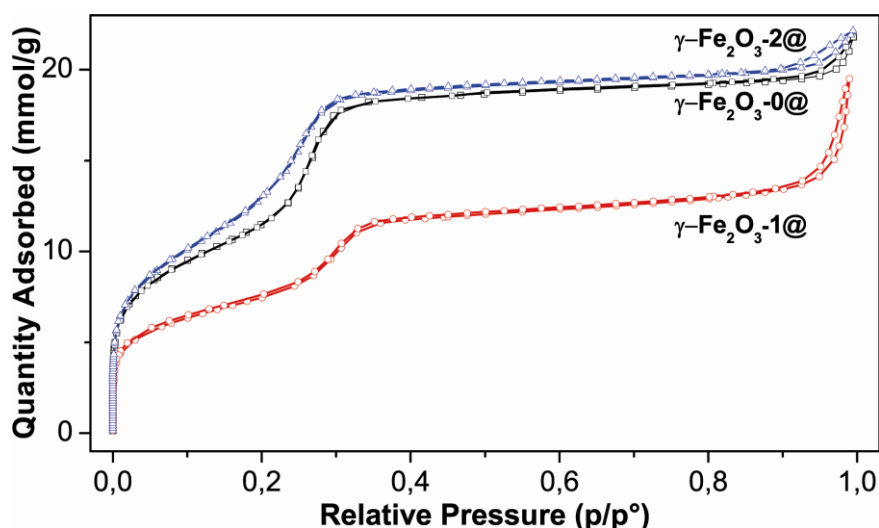


Figure S3. Nitrogen adsorption/desorption isotherms of the materials after the encapsulation process

Table S1 summarizes the surface areas (S_{BET}), pore volumes (V_p) and pore diameters (ϕ_p) for the $\gamma\text{-Fe}_2\text{O}_3$ samples after encapsulation into the mesoporous silica. The obtained results are generally observed in typical MCM-41 structures, although the mesoporous structure seems to be specially distorted in $\gamma\text{-Fe}_2\text{O}_3\text{-1@}$ sample. This fact points out that $\gamma\text{-Fe}_2\text{O}_3\text{-1}$ coated nanoparticles strongly interact with the surfactant and soluble silica that eventually result in mesoporous particles during the encapsulation process.

Table S1. Textural properties determined by means of N_2 sorption porosimetry for the magnetic particles after the encapsulation process.

Sample	S_{BET} (m^2/g)	V_p (cm^3/g)	ϕ_p (nm)
$\gamma\text{-Fe}_2\text{O}_3\text{-0@}$	945	0.7	3.1
$\gamma\text{-Fe}_2\text{O}_3\text{-1 @}$	607	0.7	4.1
$\gamma\text{-Fe}_2\text{O}_3\text{-2 @}$	1216	0.7	1.5

ϕ_p : pore diameter, V_p : pore volume, S_{BET} : surface area

Inductive coupled plasma (ICP) elemental analysis

The chemical composition of the encapsulated particles was investigated by inductive coupled plasma (ICP) elemental analysis using a Varian-Vista AxPne spectrometer.

Table S2. Maghemite content (% in weight) for synthesized samples.

Sample	$\gamma\text{-Fe}_2\text{O}_3$ (%w/w)
$\gamma\text{-Fe}_2\text{O}_3\text{-0}$	100
$\gamma\text{-Fe}_2\text{O}_3\text{-0@}$	10.68
$\gamma\text{-Fe}_2\text{O}_3\text{-1@}$	15.02
$\gamma\text{-Fe}_2\text{O}_3\text{-2@}$	7.08

Results obtained from Rietveld refinements for all the samples considered in this study.

Table S3. Lattice parameters, (Fe)-O-[Fe] distances and angles, and calculated formula parameters obtained from Rietveld refinements for maghemite phase. (Fe) and [Fe] indicate Fe³⁺ cations in tetrahedral and octahedral sub-lattices, respectively, and □ means vacancies.

Sample	a (Å)	(Fe)-O-[Fe] distance (Å)	(Fe)-O-[Fe] angle	Formula ^a
γ-Fe ₂ O ₃ -0	8.3552 (8)	3.464 (0)	123.9 (2)	(Fe) _{0.83} (□) _{0.17} [Fe] _{1.55} [□] _{0.12} O ₄
γ-Fe ₂ O ₃ -0@	8.3460 (10)	3.460 (0)	124.2 (4)	(Fe) _{0.83} (□) _{0.17} [Fe] _{1.34} [□] _{0.33} O ₄
γ-Fe ₂ O ₃ -1@	8.3486 (11)	3.461 (0)	124.3 (2)	(Fe) _{0.90} (□) _{0.10} [Fe] _{1.50} [□] _{0.17} O ₄
γ-Fe ₂ O ₃ -2@	8.3706 (32)	3.470 (1)	123.0 (6)	(Fe) _{0.84} (□) _{0.16} [Fe] _{1.48} [□] _{0.19} O ₄

^a Calculated from refined occupancy factors. (Fe)[Fe]_{1.67}O₄ is considered as stoichiometric formula for maghemite

The Rietveld refinements of XRD patterns provide valuable information about the crystalline and microstructural characteristic of maghemite nanoparticles inside the silica spheres. The molecular formulas obtained from the occupancy factors after Rietveld refinement, indicate that both γ-Fe₂O₃ nanoparticles before and after encapsulation are not stoichiometric and contain more vacancies than the expected for stoichiometric one. Even more, contrarily to the standard maghemite, our maghemite nanoparticles also have vacancies at the tetrahedral sites. This excess of vacancies indicates the presence of lattice hydrogen. From the electroneutrality law, the compositions were established to be Fe_{2.38}H_{0.86}O₄, Fe_{2.17}H_{1.49}O₄, Fe_{2.40}H_{0.80}O₄ and Fe_{2.32}H_{1.04}O₄ for γ-Fe₂O₃, γ-Fe₂O₃-0@, γ-Fe₂O₃-1@, and γ-Fe₂O₃-2@, respectively. Taking into account the nanosized microstructure of both maghemites, most of the lattice hydrogen should be placed at the nanoparticles surface.

Determination of microstructural characteristic by Rietveld refinements using FullProf

In the Rietveld refinement performed with FullProf, the program reads the instrumental resolution function of the diffractometer to get microstructural parameters from the studied sample. The instrumental resolution function (IRF) of the diffractometer was obtained from a well crystallized LaB₆ standard sample and taken into account in a separate input file. A pseudo-Voigt profile function was used with an asymmetry correction at low angle.

The refinement of the appropriate size and strains, using different models, automatically provides an output file with the apparent sizes and strains along the different $[hkl]^*$ reciprocal directions. In this case, an isotropic model (spherical crystal) was introduced

Table S4. Microstructural parameters (crystal size and strain) and agreement factors obtained from Rietveld refinements for maghemite phase.

Sample	Crystal size ^a (nm)	Maximum strain ^a (%)	Rp	Rwp	R _{Bragg}	χ^2
$\gamma\text{-Fe}_2\text{O}_3\text{-0}$	8.12 (1)	16.72 (1)	9.75	14.5	5.12	1.27
$\gamma\text{-Fe}_2\text{O}_3\text{-0@}$	9.89 (8)	32.61 (2)	6.60	9.43	6.99	1.13
$\gamma\text{-Fe}_2\text{O}_3\text{-1@}$	9.82 (1)	39.43 (3)	8.17	11.7	5.61	1.16
$\gamma\text{-Fe}_2\text{O}_3\text{-2@}$	8.49 (6)	29.25 (2)	6.16	8.75	10.9	1.15

^a The standard deviations appearing in the global average apparent size and strain are calculated using the different reciprocal lattice directions. It is a measure of the degree of anisotropy, not of the estimated error.